Supporting Information

An electrothermal platform for active droplet manipulation

Content

1. Supplementary Figures: Figure S1-S12

2 Supplementary Movies

Supplementary Movie S1. Temperature change of WS-SLIPS under

loading/unloading Joule heat (Voltage: 12 V).

Supplementary Movie S2. Climbing of liquid paraffin on droplet surface.

Supplementary Movie S3. A multi-droplet fueling strategy.

Supplementary Movie S4. Extended application of WS-SLIPS with special shapes.

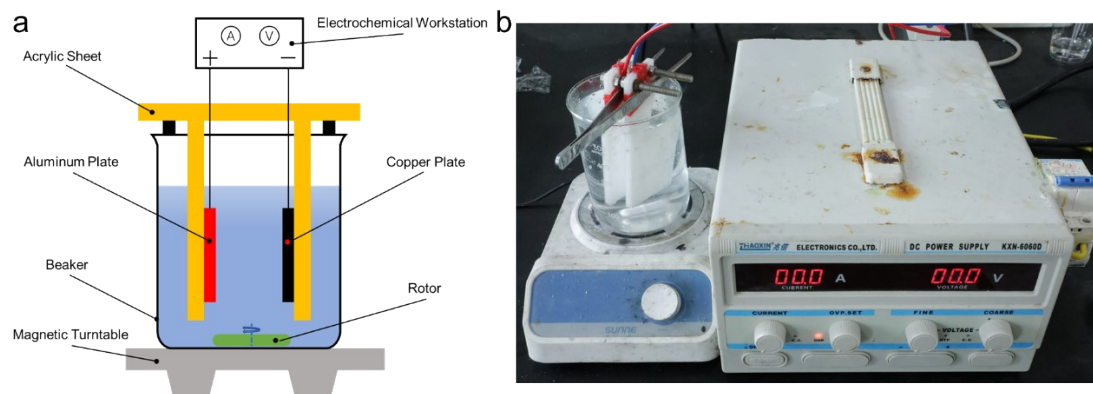Supplementary Movie S5. Self-healing capability of WS-SLIPS.

1. Supplementary Figures

Figure S1. Equipment of electrochemical processing and anodizing (a) Schematic. (b) physical diagram.

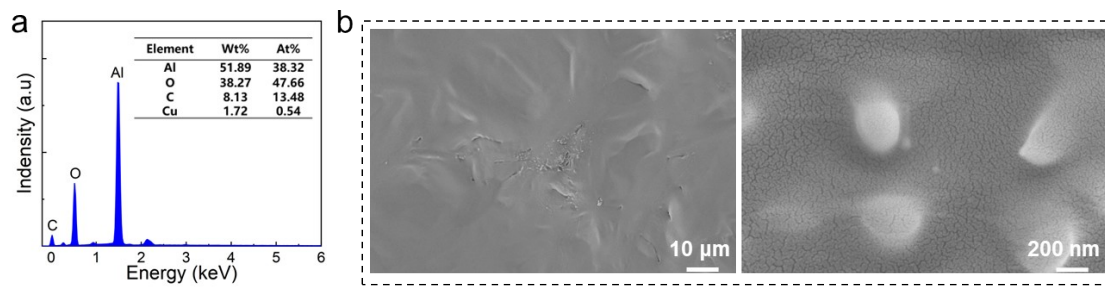| Element	Wt%	At%
Al	51.89	38.32
O	38.27	47.66
C	8.13	13.48
Cu	1.72	0.54

Figure S2. Characterization of WS-SLIPS. (a) Elements of WS-SLIPS after anodic oxidation treatment. (b) SEM of WS-SLIPS of porous structures infused by solid paraffin.
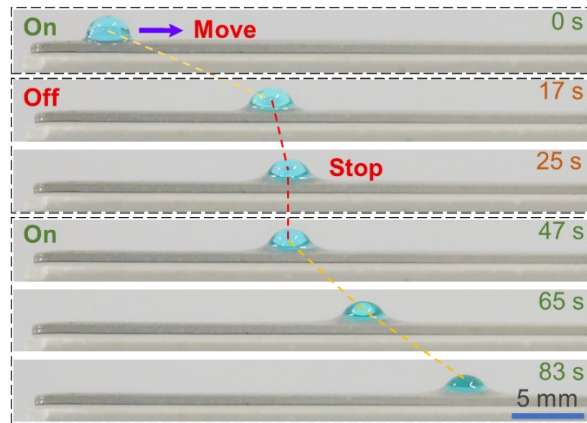
Figure S3. The WS-SLIPS with α = 4° allows spontaneous and controlled manipulation of droplet (~10ul) movement from the tip to the tail by adjusting voltage loading and unloading Joule heat.
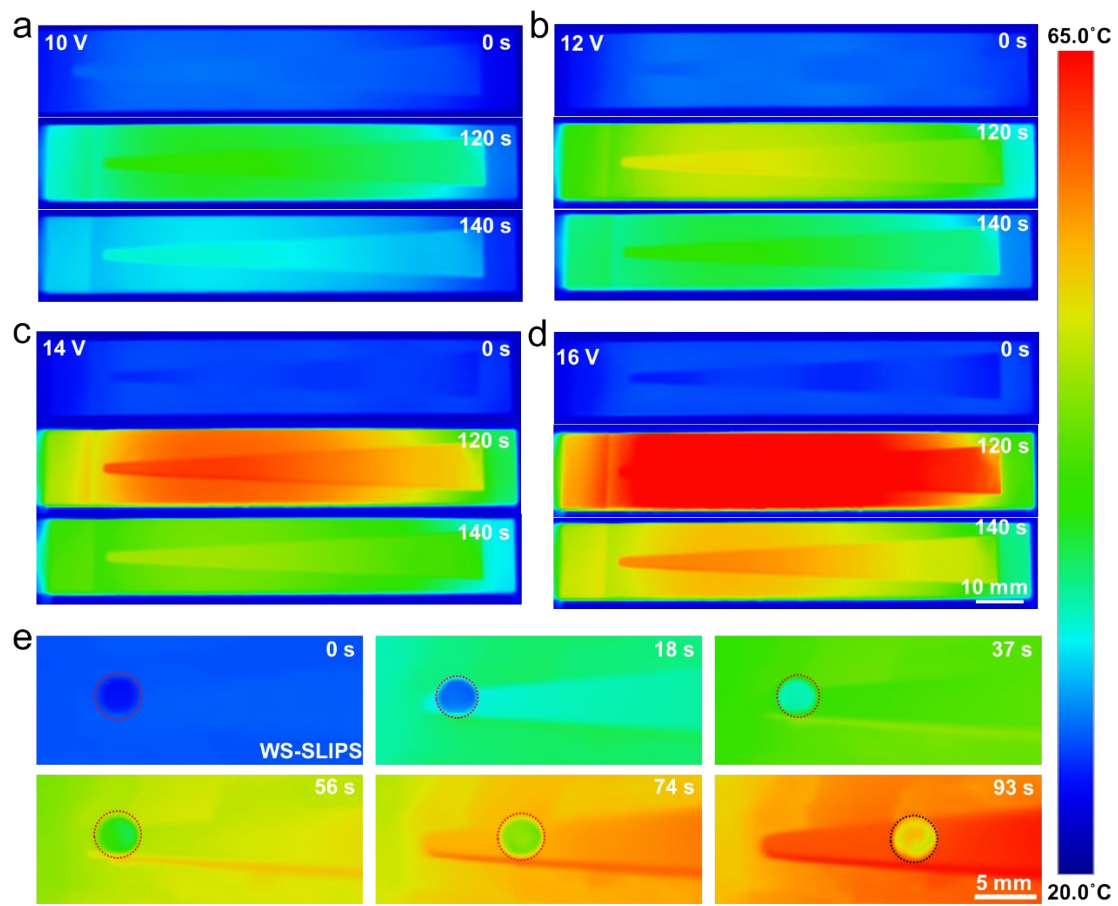
Figure S4. Thermal image of the surface temperature after loading different voltage for 120 s and after unloading voltage for 20 s. (a) 10 V. (b) 12 V. (c) 14 V. (d) 16 V. (e) Thermal image of the WS-SLIPS's temperature change after loading a voltage of 16 V.
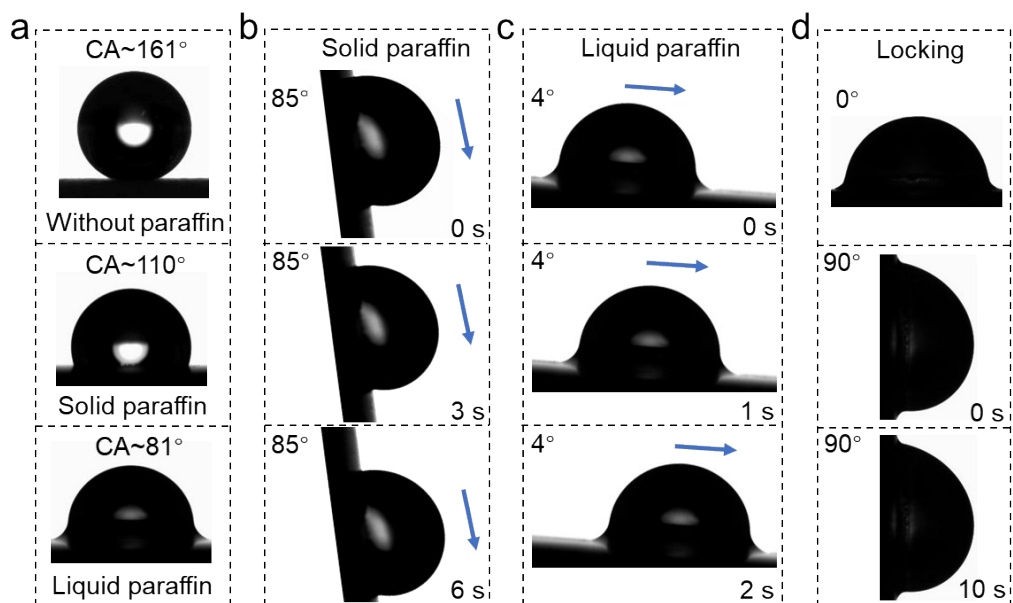
Figure S5. Determination of CAs and SAs of droplets (~5 μl) on WS-SLIPS in different states. (a) CAs of droplets on WS-SLIPS without paraffin infusion, falling on the surface of solid paraffin and on WS-SLIPS with Liquid paraffin. (b) SA of droplet on WS-SLIPS surface with solid paraffin. (c) SA of droplet on WS-SLIPS surface with liquid paraffin. (d) Measurement of SA when paraffin is converted from liquid to solid and the droplet is locked to the WS-SLIPS surface by the solid paraffin wrapping.
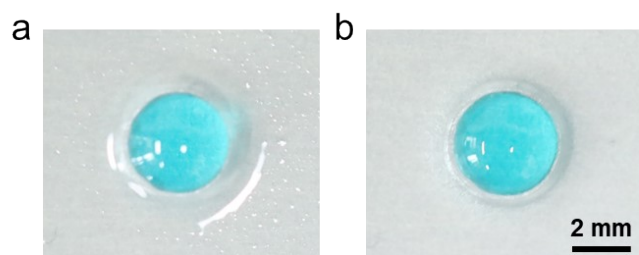
Figure S6. Images of (a) a droplet at a sliding interface and spreading on WS-SLIPS before paraffin solidification and (b) droplet locking on WS-SLIPS after paraffin solidification.
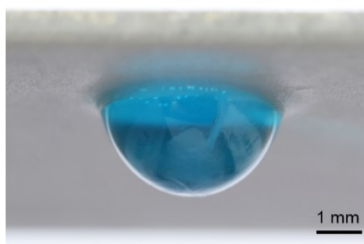
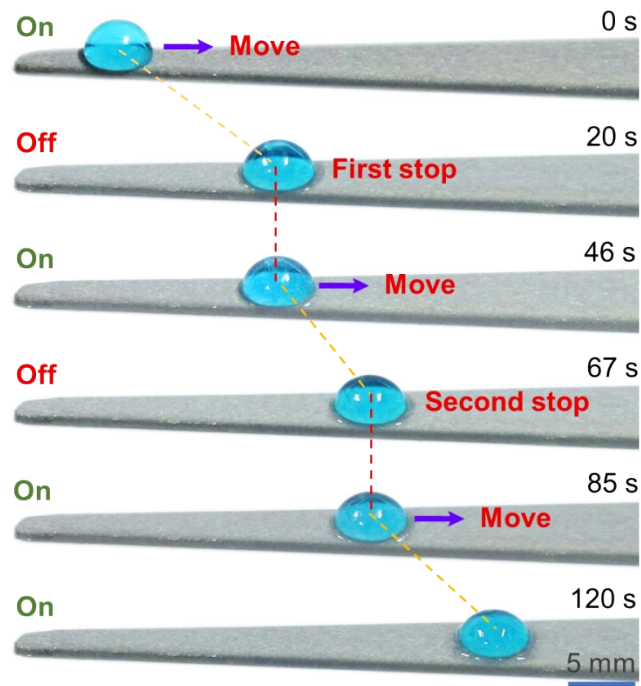Figure S7. Droplets in the "locking state" when tilted by 180°.

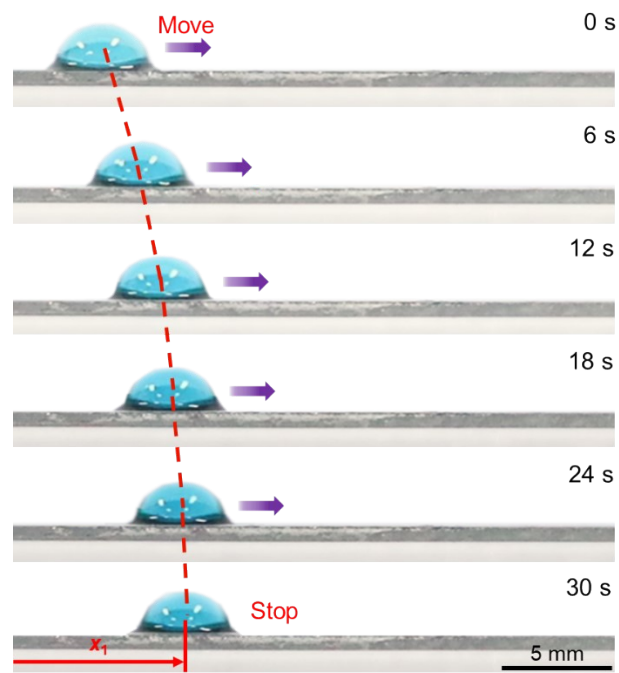Figure S8. Optical images of two droplet manipulation experiments on WS-SLIPS with $\alpha = 6°$.

Figure S9. Transport distance of x_1 for a constant volume single droplet on WS-SLIPS.
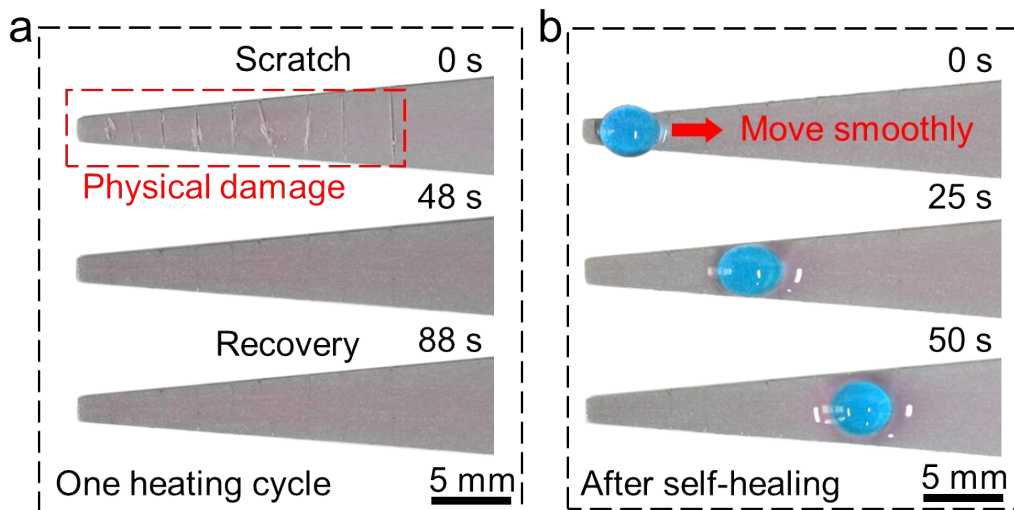
Figure S10. Self-healing of WS-SLIPS. (a) The damaged surface is repaired after a heating cycle. (b) Droplet transport can still be realized on the surface after self-healing.
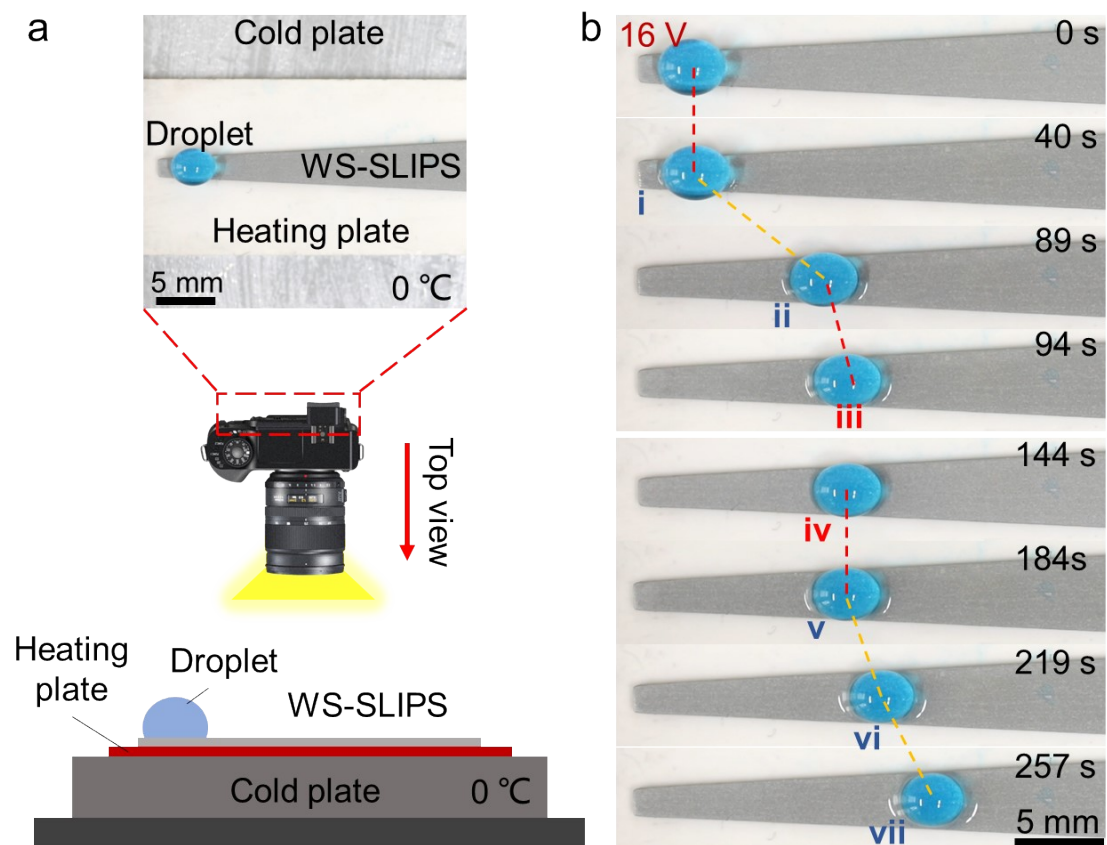
Figure S11. Droplet manipulation experiments at low temperature. (a) Schematic diagram of experiment equipment; (b) Optical image of droplet manipulation process.
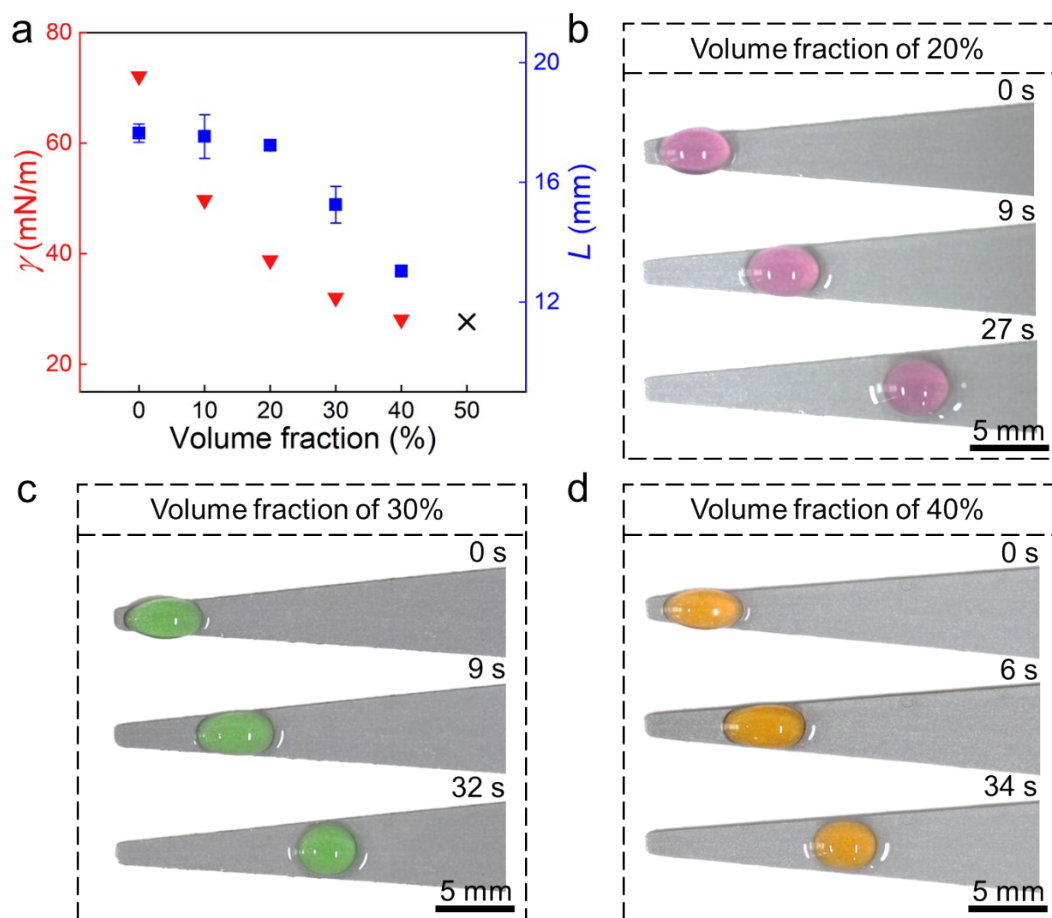
Figure S12. Transport process of droplets with different surface tension on WS-SLIPS. (a) surface tension and transport distance of ethanol solutions with different volume fractions. Optical images of ethanol solutions with (b) volume fractions of 20%, (c) volume fractions of 30% and (d) volume fractions of 40% transported on WS-SLIPS.